Design and Implementation of Digital Fractional Order PID Controller using Optimal Pole-Zero Approximation Method for Magnetic Levitation System

Amit S. Chopade, Swapnil W. Khubalkar, A. S. Junghare, M. V. Aware, and Shantanu Das

***Abstract*—The aim of this paper is to employ fractional order proportional integral derivative (FO-PID) controller and integer order PID controller to control the position of the levitated object in a magnetic levitation system (MLS), which is inherently nonlinear and unstable system. The proposal is to deploy discrete optimal pole-zero approximation method for realization of digital fractional order controller. An approach of phase shaping by slope cancellation of asymptotic phase plots for zeros and poles within given bandwidth is explored. The controller parameters are tuned using dynamic particle swarm optimization (dPSO) technique. Effectiveness of the proposed control scheme is verified by simulation and experimental results. The performance of realized digital FO-PID controller has been compared with that of the integer order PID controllers. It is observed that effort required in fractional order control is smaller as compared with its integer counterpart for obtaining the same system performance.**

***Index Terms*—Digital control, Position control, Fractional calculus, Particle swarm optimization (PSO), Approximation methods, Magnetic levitation, Discretization, Fractional order PID controller (FOPID).**

I. Introduction

IN 1914, American inventor Emile Bachelet presented his idea of a magnetically levitated (maglev) vehicle with a display model. In magnetic levitation system (MLS), ferromagnetic object levitate by the electromagnetic force induced due to electric current flowing through coil around a solenoid[1−5]. The MLS is inherently nonlinear and unstable[6−10]. However, the advantage is that, as the suspended object has no mechanical support, there is no friction and noise. This allows us to position it accurately - a major advantage, explored in many applications such as magnetically levitated train, magnetic bearing, conveyor system, etc.[1].

In recent years, various methods have been proposed to improve control in MLS-based applications. In 2006, Chiang et al. proposed the concept of integral variable-structure grey control[2]. Yang et al. introduced the concept of adaptive robust output-feedback control with K-filter approach in 2008[3]. In 2011, Chih-Min Lin et al. developed an adaptive PID controller and a fuzzy compensation controller for MLS[1]. In the same year, Rafael Morales et al. proposed generalized proportional integral output feedback controller[4]. Recently in 2014, Chih-Min Lin et al. proposed a function-link cerebellar model articulation control system design based on the neural network concept[5]. However, in spite of all these developments, there is scope for improving efficiency of the controller. The energy required to achieve and maintain the object's position (in the face of disturbances) form an important part of improving the control action. The aim of this paper is to control and maintain the desired object's position, with lesser controller effort. The controller effort minimization is reported in literature[11−14].

The conventional integer order controllers such as, PD and PID controller have been applied in industry for over half-a-century to control linear and nonlinear systems[15]. Recently, such control schemes have been extended to their generalized form using fractional calculus[16−17] (differentiation and integration of an arbitrary order). The FO-PID controller has fractional differ-integrator operations. This makes the controller have memory (i.e. its action will memorize its past states) and avoids instantaneous actions. Using the definition of convolution integral, the expression for the fractional integration (which also is embedded in the fractional differentiation) can be written as the convolution of the function and the power function, which is elaborately explained in [17].

In last few decades, the fractional order approach to represent the plant and its controllers are increasingly used to describe the dynamic process accurately[17]. The fractional order transfer function is approximated by integer order transfer function using various methods[16−20]. The proposed method can achieve the desired accuracy over a much larger bandwidth than has been achieved using earlier methods. In applications, where non-integer order controllers are used for integer order

This article has been accepted for publication in a future issue of this journal, but has not been fully edited. Content may change prior to final publication.

This work was supported by the Board of Research in Nuclear sciences of the Department of Atomic Energy, India. Sanction no. 2012/36/69-BRNS/2012. Recommended by Associate Editor Antonio Visioli.

Amit S. Chopade, Swapnil W. Khubalkar, Anjali S. Junghare, and Mohan V. Aware are with the Department of Electrical Engineering, Visvesvaraya National Institute of Technology, Nagpur, India 440010 e-mail: (a.s.chopade@ieee.org, swapnil.w.khubalkar@ieee.org, asjunghare@eee.vnit.ac.in, mvaware@eee.vnit.ac.in).

Shantanu Das is with Reactor Control Division, Bhabha Atomic Research Centre, India. e-mail: (shantanu@barc.gov.in).

Digital Object Identifier 10.1109/JAS.2016.7510181

plant, there is more flexibility in adjusting the gain and phase characteristics as compared to integer order controllers. This flexibility makes fractional order control a more versatile tool in designing robust and precise control systems.

This paper presents the control of magnetic levitation system using FO-PID controller based on optimal pole-zero approximation method. An algorithm is developed to realize digital FO-differentiators and FO-integrators. The proposed design procedure aims to ensure that the performance is within required tolerance bandwidth. Five parameters $(k_p, k_i, k_d, \alpha, \beta)$ of FO-PID need to be tuned for designing the controller. This paper utilizes dynamic PSO optimization (dPSO) method to achieve the required values. Finally, a comparative study of the performance parameters of the controller is presented to evaluate the advantages of deployment of FO-PID against the conventionally used integer-order controllers. The control effort minimization by FO-PID controller is quantified and demonstrated.

This work is organized as follows: section II presents the system description. Design procedure of proposed digital FO-PID controller using discrete optimal pole-zero approximation method and dPSO technique is discussed in section III. In section IV simulation and experimental results on MLS are provided to validate effectiveness of the proposed controller. Paper concludes with a summary of the results obtained in section V.

II. System Identification of MLS Model

A laboratory scale magnetic levitation system is used to evaluate the performance of proposed controller in a controlled environment. MLS levitates an object (metallic ball with mass m) in a desired position by controlling the electromagnetic field counteracting the gravitational force. The applied control input is voltage, which is converted into current via embedded driver[21]. Fig.1 shows the schematic diagram of MLS. The system model is nonlinear, that means at least one of the two states (i–current, x–ball position) is an argument of a nonlinear function. The nonlinear model of MLS relating the ball position x and coil current i is given as (1):

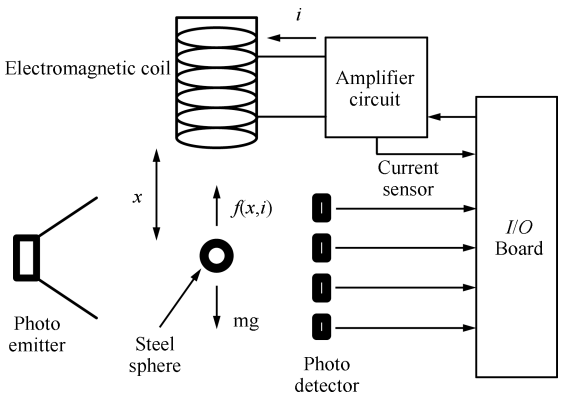

Fig. 1. Schematic diagram of MLS.

$$m\ddot{x} = mg - k\frac{i^2}{x^2} \tag{1}$$

$$i = k_1 u \tag{2}$$

where, k is a constant depending on coil (electromagnet) parameters, m is the mass of sphere, g is gravitational force, k_1 is an input conductance, u is control voltage, and x is a ball position. The values of these parameters are given in Appendix-A. A relation between control voltage x and coil current i is given in (2). The control signal ranges between $[-5V, +5V]$.

A. Linearization of MLS Model

The nonlinear form of maglev model is linearized for analysis of the system[21]. The linear form of the model is obtained from (1) as follows:

$$\ddot{x} = g - f(x, i) \tag{3}$$

where, $f(x,i) = k\frac{i^2}{mx^2}$
Equilibrium point is calculated by setting $\ddot{x} = 0$,

$$g = f(x, i)|_{i_o, x_o} \tag{4}$$

Linearization is carried out about the equilibrium point of $x_o = -1.5V$ (the position is expressed in volts), $i_o = 0.8A$[8]. Using series expansion method, (5) is obtained.

$$\ddot{x} = -\Big(\frac{\partial f(i,x)}{\partial i}\Big|_{i_o,x_o} \triangle i + \frac{\partial f(i,x)}{\partial x}\Big|_{i_o,x_o} \triangle x\Big) \tag{5}$$

Application of Laplace Transform on (5) simplifies it to (6).

$$\frac{\triangle X(s)}{\triangle I(s)} = \frac{-K_i}{s^2 + K_x} \tag{6}$$

where, $K_i = \frac{2mg}{i_o}$ and $K_x = -\frac{2mg}{x_o}$

Linearized model transfer function (6) has two poles, one of which is in the right half plane at $\sqrt{(2mg/x_0)}$, which makes the MLS open-loop unstable. Transfer function, obtained by the linearization, is verified using system identification procedure.

B. Integer Order System Identification of MLS Model

System identification is a process for obtaining mathematical model using input and output system response. The identified model response should fit with measured response for input applied to the system model[21]. Usually there are two methods for system identification, least mean square (LMS) method and instrumental variable method. The identification of MLS is generally accomplished via traditional least squares method, and is implemented in MATLAB[21−22].

As MLS is unstable, it has to be identified with a running, stabilizing controller i.e. closed loop identification. Fig.2 shows the scheme of unstable system identification. LMS method minimizes error between the model and plant output. The optimal model parameters, for which the square of the error is minimal is the result of identification. In order to carry out identification experiment, a discrete controller has to be applied, in the absence of which, the ball falls down,

rendering dentification impossible. The reference signal $r(t)$ i.e. random binary sequence signal is given to excite the MLS and output $y(t)$ is monitored. 2500 samples of the input, output signals are collected from the system with sampling period of $0.01s$.

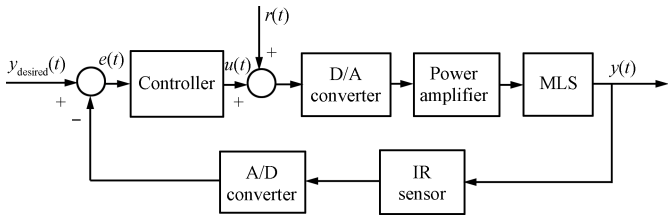

Fig. 2. Block diagram of MLS control and close loop system identification.

Fig.3 presents the comparison between measured and identified model output. Input and output data is taken from MLS system for real-time identification. The best fit obtained is 90.78% for integer order identification, which gives close loop discrete transfer function as in (7):

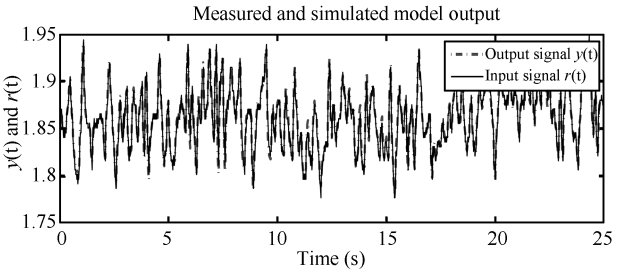

Fig. 3. Measured and simulated model output.

$$Y(z^{-1}) = \frac{G(z^{-1})}{1 + C(z^{-1})G(z^{-1})} \tag{7}$$

where, $Y(z^{-1})$ is complete system transfer function, $C(z^{-1})$ is controller transfer function, and $G(z^{-1})$ is MLS model transfer function in discrete domain.

III. DESIGN OF DIGITAL FRACTIONAL ORDER PID CONTROLLER

A. Fractional Calculus

Fractional calculus is a branch of mathematics that studies the possibility of taking real or complex number powers of differential and integral operator. Basic definitions of fractional calculus and approximation of fractional integrator and fractional differentiator are described in the literature[16−17]. The real order operator is generalized as follows in (8):

$$D^{\alpha} = \left\{ \begin{array}{cc} \frac{d^{\alpha}}{\mathrm{d}t} & \alpha > 0 \\ 1 & \alpha = 0 \\ \int_a^t (\mathrm{d}\tau)^{-\alpha} & \alpha < 0 \end{array} \right\} \tag{8}$$

where, $\alpha \in \mathbf{R}$

Some popular definitions used for general fractional derivatives/integrals in fractional calculus are :

1) : Riemann-Liouville (RL) definition is given in (9).

$${}_aD_t^{\alpha} f(t) = \frac{1}{\Gamma(n-\alpha)} \left(\frac{\mathrm{d}}{\mathrm{d}t}\right)^n \int_a^t \frac{f(\tau)}{(t-\tau)^{\alpha-n+1}} \mathrm{d}\tau \tag{9}$$

for $(n-1) \leq \alpha < n$

where, n is an integer, α is a real number, and Γ is Euler gamma function. Laplace transform of the RL fractional derivative/integral (9), under zero initial conditions, is given in (10).

$$L\{{}_aD_t^{\pm\alpha} f(t)\} = s^{\pm\alpha} F(s) \tag{10}$$

2) : Another definition is based on the concept of fractional differentiation i.e. Grunewald-Letnikov (GL) definition. It is given in (11).

$${}_aD_t^{\alpha} f(t) = \lim_{h \to 0} h^{-\alpha} \Sigma_{j=0}^{\left[\frac{t-a}{h}\right]} (-1)^j \binom{\alpha}{j} f(t-jh) \tag{11}$$

where, $\left[\frac{t-a}{h}\right] \longrightarrow Integer$

3) : One more option for computing fractional derivatives is Caputo fractional derivative, its definition is as follows (12):

$${}_a^C D_t^{\alpha} f(t) = \frac{1}{\Gamma(n-\alpha)} \int_a^t \frac{f^n(\tau)}{(t-\tau)^{\alpha+1-n}} \mathrm{d}\tau \tag{12}$$

where, $(n-1) \leq \alpha < n$, n is an integer, and α is a real number.

Initial conditions for Caputo's derivatives are expressed in terms of initial values of integer order derivatives. It is noted that for zero initial conditions RL, GL, and Caputo fractional derivatives coincide. Hence, any of the mentioned methods may be used, using the case of zero initial conditions. That would then eliminate the differences arising due to different initial conditions (amongst the three methods).

B. Digital Realization of Fractional Order Differintegrals with Optimal Pole-Zero for Phase Shaping

The aim behind the choice of frequency domain rational approximation of FO-PID controller is to realize the controller in real time using existing analog/digital filters[16−20, 23−25]. Precise hardware implementation of multi-dimensional natured of fractional order operator is difficult. However, recent research work revealed that band-limited implementation of FO-PID controllers using higher order integer transfer function approximation of the differintegrals give satisfactory performance[26]. This paper, hence utilizes optimal pole-zero algorithm to realize fractional differintegrals in the frequency domain.

1) Optimal pole-zero approximation for phase shaping: Any rational transfer function is characterized by its poles and zeros. The Bode magnitude plot of non-integer order transfer function has a slope of $\pm\alpha 20$ dB/dec and the Bode phase plot lies in the range of $\pm\alpha 90^o$ (α is a real number). This is achieved by the interlacing of real poles and zeros alternately on the negative real axis[19−20, 27−28]. Thus, depending on the error band ϵ around required phase angle $\alpha_{req} = \alpha 90^o$

and the frequency band of interest (ω_L, ω_H), the n^{th} order approximation is obtained[28]. The proposed algorithm is developed to obtain the number of optimal pole-zero pairs to maintain the phase value within the tolerance, of around 1^o. In this algorithm, poles and zeros given by (13) are obtained as follows:

$$\begin{aligned} First\ pole,\ p_1 &= 10^{[\frac{\phi_{req}+45log\omega_l}{45}+1]} \\ First\ zero,\ z_1 &= 10\omega_l \\ Second\ pole,\ p_2 &= 10^{[log(p_1)+2-\mu]} \\ Second\ zero,\ z_2 &= 10^{[log(z_1)+2-\mu]} \\ &\vdots \\ till\ p_n &\geq \omega_h \end{aligned} \tag{13}$$

As a particular case, asymptotic phase plot for fractional order integrator circuit having $\alpha = -0.4$, $\phi_{req} = -36^o$, $\omega_L = 0.1$rad/s and $\omega_H = 100$rad/s is given in Fig.4 - Fig.6. The selection of three pairs of poles and zeros with $\alpha = -0.4$ fraction is shown in Fig.4. The asymptotic phase plot is a straight line at ϕ_{req}, but the actual phase plot is oscillating about asymptotic phase plot, apart from that the average value of phase angle -37.31^o is also different from ϕ_{req}. In Fig.4 the required correction of phase is achieved over three decades by three pole-zero pairs only, which is however less in pursuit of more accuracy. This problem is rectified by increasing the pole-zero density, i.e. having more pole-zero pairs in the desired frequency band. Number of pole-zero pairs depend on the permissible error and the desired band of frequency.

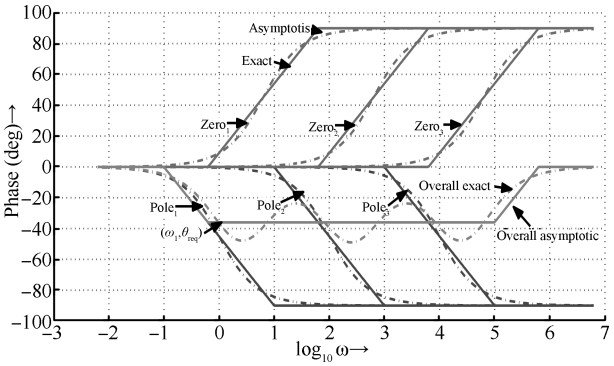

Fig. 4. Asymptotic phase plot with three pole-zero pairs for $\alpha = -0.4(-36^o)$.

Generally, three pole-zero pairs per decade give the phase plot within $\varepsilon = \pm 1^o$ error, but it depends on the value of α as well. For the same parameters, i.e. $\alpha = -0.4, \phi_{req} = 36^o$, $\omega_L = 0.1$rad/s and $\omega_H = 100$ rad/s with seven pole-zero pairs, phase plot is shown in Fig.5. The actual phase plot is oscillating with rms error of $0.6471^o (< 1^o)$. Apart from that, average value of phase angle $(-35.9999^o \approx -36^o)$ is same as ϕ_{req}. Moreover, this is achieved over 3 decades of cycle by seven pole-zero pairs. In order to maintain the phase margin tolerance within the lower limits, more pole-zero pairs in the desired frequency band are required. This can be done by adjusting z_1, p_2, z_3.... closer towards left. To achieve this shift, design parameter μ is introduced. Frequency band of constant phase shrinks on both the ends with increasing μ for constant number of pole-zero pairs. Fig.6 shows the basic idea of frequency band tightening. The problem regarding frequency band shrinking is tackled by designing the rational approximation on wider frequency band $(\frac{\omega_l}{10^\gamma}, 10^\delta \omega_h)$ followed by curtailing the frequency overhang on either side, such that the phase remains within $\phi_{req} \pm \varepsilon$ in range of (ω_l, ω_h). Nominal values to expand frequency band are $\gamma = 3, \delta = 2$.

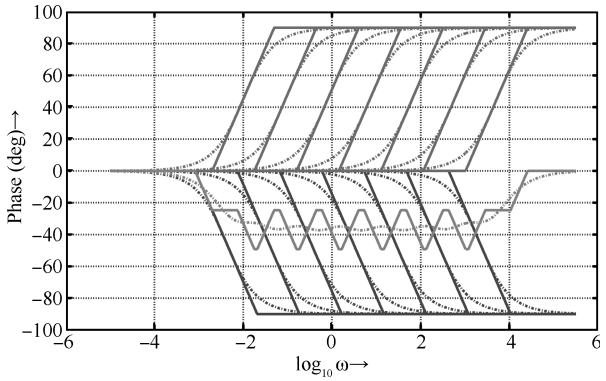

Fig. 5. Asymptotic phase plot with seven pole-zero pairs.

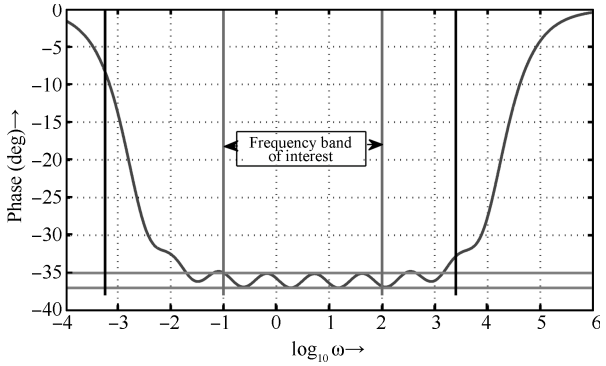

Fig. 6. The basic idea of frequency band tightening.

2) Design of Digital Fractional Order Integrator: The key point in digital implementation of fractional order controller is discretization of fractional order differintegral[24, 27−29]. Contributions related to the discretization have been reported in literature[30−33]. The pole-zero pairs obtained by algorithm in the above case are discretized using first order hold (foh), zero order hold (zoh), Tustin operator, impulse invariant, matched pole-zero, and Tustin with pre-warp frequency methods. In Fig.7, Bode plot for $s^{-0.4}$ digital integrator is shown and it depicts that digital integrator with Tustin approximation method matches closely with continuous time integrator. Tustin approximation method with a sample time of $0.01s$ is used for discretization. To relate s-domain and z-domain transfer functions, Tustin and bilinear methods use the following approximation as (14).

$$z = e^{sT_s} \approx \frac{1 + sT_s/2}{1 - sT_s/2} \tag{14}$$

The optimal pole-zero algorithm for digital fractional integrator of $s^{-0.4}$ within desired band of frequency $\omega_L = 0.1$rad/s and $\omega_H = 100$rad/s gives pole-zero pairs which are listed in Table 1 with gain value 0.010127.

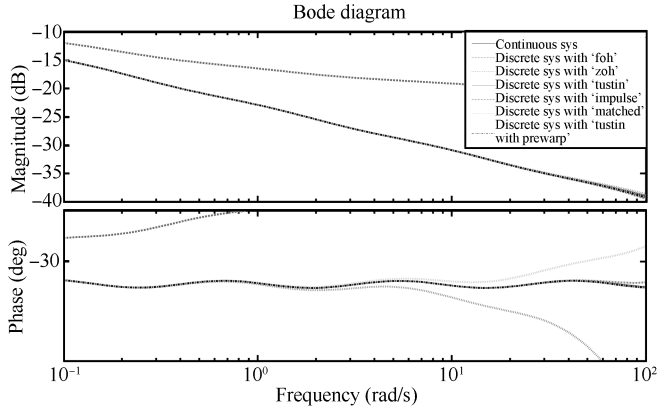

Fig. 7. Bode plot of $s^{-0.4}$ digital integrator.

Table I
THE POLE-ZERO PAIRS OF THE RATIONAL APPROXIMATION OF $s^{-0.4}$ ON $(10^{-1}, 10^{2})rad/s$

i	1	2	3	4	5	6	7
z_i	−0.9253	−0.4842	0.9307	0.992	0.9991	1	0.5136
p_i	−0.8286	0.7651	0.9707	0.9967	1	1	−0.0875

Digital fractional differentiator is designed along the lines of approach similar to that of digital fractional integrator. The architecture of digital FO-PID with digital fractional integrator and digital fractional differentiator is shown in Fig.8.

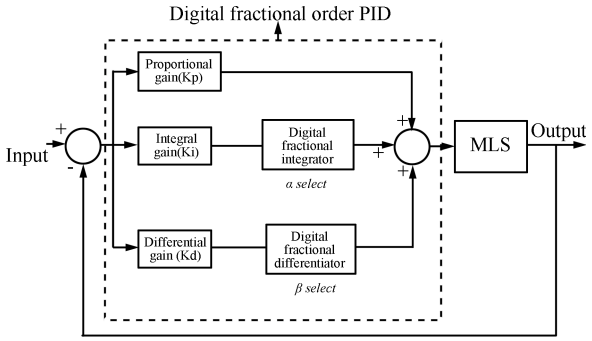

Fig. 8. Digital FO-PID controller.

3) dynamic Particle Swarm Optimization: Recently, many researchers have focused on fractional order controllers tuning, and have obtained meaningful results[34−47]. In this work, dPSO method is used to tune the gains and orders of the controller. PSO is a method for optimizing hard numerical functions, analogous to social behavior of flocks of birds, schools of fish, etc. Here, each particle in swarm represents a solution to the problem defined by its instantaneous position and velocity[48]. The position vector of each particle is represented by unknown parameters to be ascertained. In present case, five control parameters $(k_p, k_i, k_d, \alpha, \beta)$ of FO-PID controller need to be ascertained. The desired number of particles is known as population. The population is varied to carry out a search in multidimensional space. Each particle in population will travel with the updated velocity and direction to converge as early as possible to the optimal solution point. Dynamic PSO is an improvement in PSO by adding the product of differences in objective function value between a particle and its individual best or the global best. Here, the change in position of a particle is directly proportional to iteration, which further depends on individual best, global best, and a random velocity[49]. dPSO searches the workspace similar to a simple PSO and velocity of a particle is obtained by (15):

$$\begin{aligned} v_{id} = {} & (f(p_{id}) - f(x_{id})) \times (p_{id} - x_{id}) \times sf_1 \\ & + (f(p_{gd}) - f(x_{id})) \times (p_{gd} - x_{id}) \times sf_2 \\ & + rand() \times signis() \times sf_3 \end{aligned} \tag{15}$$

where, v_{id}: velocity of a particle, p_{id}: individual best, x_{id}: current position of a particle, p_{gd}: global best, rand: random function, sf_1, sf_2, sf_3: to scale the calculated value in the range of the control variable, $signis$: function which generates random positive or negative value.

Population size is taken as 100, maximum iteration is set as 50, lower and higher translation frequencies are taken as $\omega_L = 0.1$rad/s and $\omega_H = 100$rad/s. ITAE (Integral Time Absolute Error) is chosen as performance criterion. The values of controller parameters, obtained from dPSO, are implemented in PD, PID, and FO-PID controller in simulation as well as in real time mode on MLS. The optimized values of the controllers are presented in Table II.

Table II
dPSO OPTIMIZED GAIN AND FRACTIONAL ORDER VALUES USED FOR DIFFERENT CONTROLLERS (α :ORDER OF INTEGRATOR, β :ORDER OF DIFFERENTIATOR)

Sr. No.	Controllers	Gain and Fractional Order Value				
		K_p	K_i	K_d	α	β
1.	**PD**	4	–	2	–	1
2.	**PID**	5.5	2	0.2	1	1
3.	**FOPID**	7	12	1	0.4	0.8

IV. MLS CONTROL: SIMULATION AND HARDWARE

A. Closed-Loop Control System Simulation

Control of MLS using optimized PD, PID, and FO-PID controller is studied by MATLAB simulation. A sinusoidal excitation signal is used to study the effects. The controller generates a compensating control signal (based on the positional error) to achieve desired ball position. Controller parameters are tuned using dPSO method as discussed in section III-B-3. Fig.9 - Fig.11 present simulation results of the controlled output of MLS using PD, PID, and FO-PID controller respectively. Here, encircled part pointed by an arrow shows deviation between desired and actual ball position.

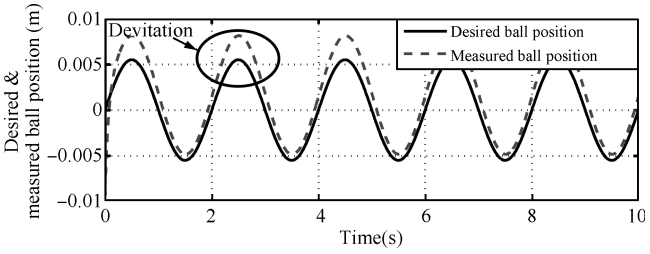

Fig. 9. Controlled output result of MLS using PD.

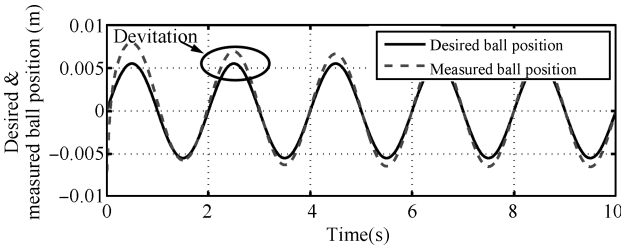

Fig. 10. Controlled output result of MLS using PID.

The measured and desired ball positions with PD, PID, and FO-PID controllers are quantitatively presented in Table III. The simulation results indicate that deviation between measured and desired ball positions by using dPSO tuned FO-PID controller, is less as compared to PD or PID controllers.

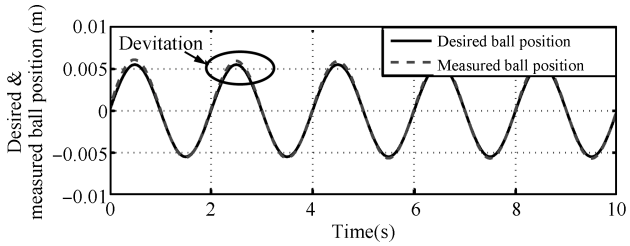

Fig. 11. Controlled output result of MLS using FO-PID.

Error values presented in Table III are calculated using (16):

$$Percent\ error = \frac{desired\ position - actual\ position}{actual\ position} \times 100\% \tag{16}$$

From the data presented in Table III, it is observed that FO-PID controller tracks the desired position more efficiently than PD or PID controllers.

B. Real Time Implementation of Closed-Loop System

The MLS used for experimentation is shown in Fig.12. Due to high nonlinearity and open-loop instability, MLS system is a very challenging plant. Assembly of MLS consists of a mechanical unit labeled A in Fig.12. Analogue control interface unit labeled A is used to transfer control signals between computing system and MLS. Advanced PCI1711 I/O card has been inserted into a PCI computer slot and connected with SCSI adapter box using SCSI cable. Mathworks software tools are used to implement control algorithm. It includes MATLAB control toolbox, real time windows workshop (RTW), real time windows target (RTWT), and visual C as programming environment. The flowchart required to obtain executable file is shown in Fig.13. RTW builds a C++ source code from the Simulink Model. C code compiler compiles and links the code to produce executable program. RTWT communicates with executable program acting as the control program and interfaces with hardware through input/output board. The block diagram of MLS close loop control is shown in Fig.14.

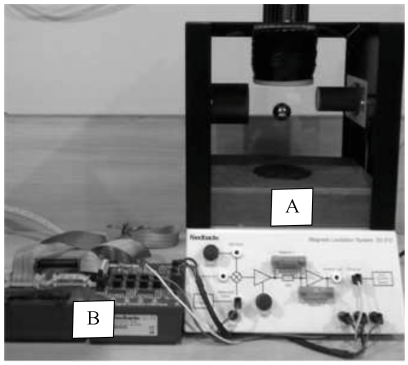

Fig. 12. Experimental setup.

1) Experimental Results using a PD Controller: The measured and desired ball positions using real time PD controller is shown in Fig.15(a) and control signal c(t) before digital to analog (D/A) conversion is given in Fig.15(b). This control signal is used to levitate the object at desired position. The plant input signal m(t) after D/A conversion and output signal y(t), captured on the digital storage oscilloscope (DSO), is presented in Fig.16.

The control effort required by controller to maintain object's position can be observed from the control signal c(t). The ball position is tracked by infrared sensor and is fed back to Simulink environment via analog to digital (A/D) converter. It is observed from Fig.15 - Fig.16 that there is more deviation in ball position and control effort required by the controller, and is higher in case of PD controller. Hence, integral action is added to the PD controller to achieve an improved control over desired ball position. The quantitative analysis of desired and actual ball position achieved by the controller is presented in Table IV and the control effort analysis of controller is shown in Table V.

Table III
MEASURED AND DESIRED BALL POSITIONS FOR DIFFERENT CONTROLLERS IN SIMULATION

Ball Positions (m)		**Controllers**		
		PD	**PID**	**FO-PID**
Measured ball position	Max.	8.12×10^{-3}	6.92×10^{-3}	5.94×10^{-3}
	Min.	-4.83×10^{-3}	-6.68×10^{-3}	-5.65×10^{-3}
Desired ball position	Max.	5.5×10^{-3}	5.5×10^{-3}	5.5×10^{-3}
	Min.	-5.5×10^{-3}	-5.5×10^{-3}	-5.5×10^{-3}
Error		23.06%	19.09%	5.03%

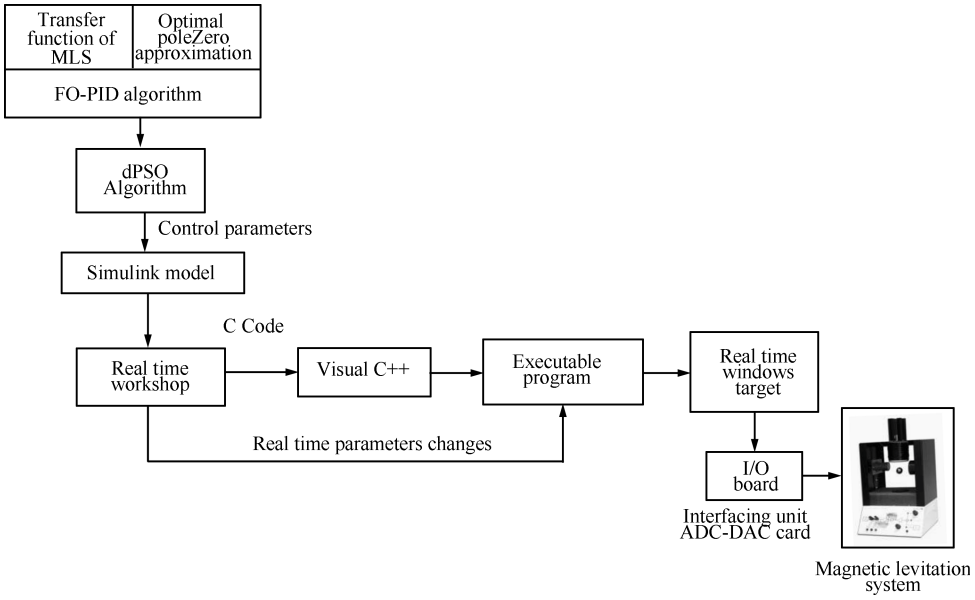

Fig. 13. Control system development flow diagram.

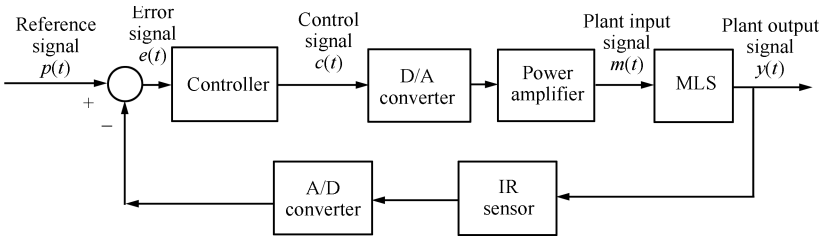

Fig. 14. Block diagram of MLS close loop control.

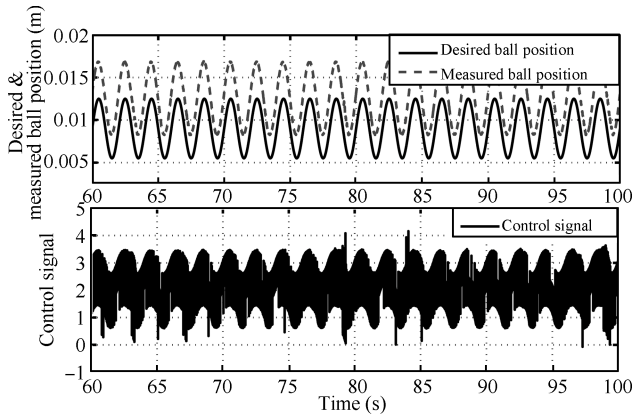

Fig. 15. (a) Controlled output result of MLS using a PD controller (b) Control signal of PD controller.

2) Experimental Results using a PID Controller: Fig.17(a) shows measured and desired ball positions using PID controller and output of controller c(t) is shown in Fig.17(b). The captured controller output signal c(t) and output signal are presented in Fig.18. The deviation in the ball position is minimized to an extent by employing the PID controller. However, the control effort required by controller is still similar to that of PD controller while achieving the improvement.

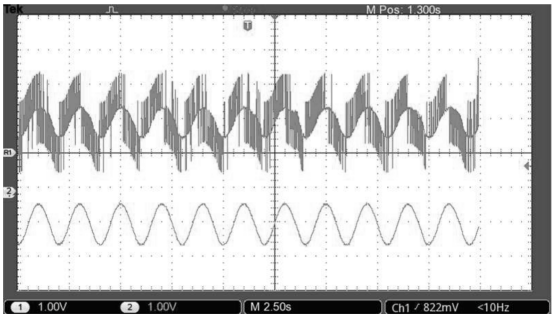

Fig. 16. Experimental PD controller output and object's trajectory captured on DSO.

3) Experimental Results using a FO-PID Controller: The deviation in ball positions using real time FO-PID controller is shown in Fig.19(a). It depicts that error in desired and actual ball positions has reduced in comparison to both PD or PID control actions. The control signal c(t) of FO-PID controller is presented in Fig.19(b). It shows that effort required by the controller is least as compared to PD or PID controllers. Plant input signal m(t) and output signal y(t) are presented in Fig.20.

Table IV
MEASURED AND DESIRED BALL POSITIONS FOR DIFFERENT CONTROLLERS IN REAL TIME IMPLEMENTATION

Ball Positions (m)		Controllers		
		PD	PID	FO-PID
Measured ball position	Max.	16.8×10^{-3}	13.1×10^{-3}	12.6×10^{-3}
	Min.	8.3×10^{-3}	4.85×10^{-3}	5.24×10^{-3}
Desired ball position	Max.	12.5×10^{-3}	12.5×10^{-3}	12.5×10^{-3}
	Min.	5.5×10^{-3}	5.5×10^{-3}	5.5×10^{-3}
Error		29.66%	8.95%	5.75%

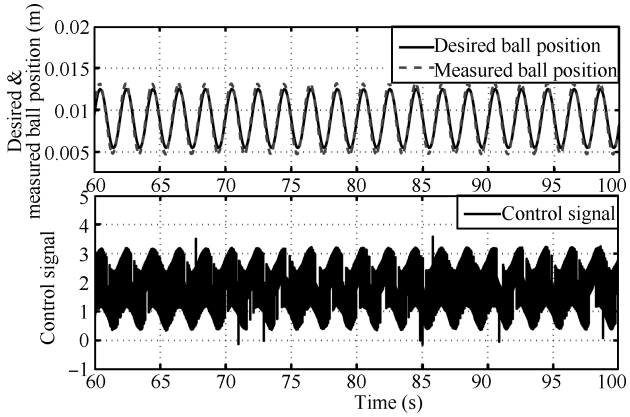

Fig. 17. (a) Controlled output result of MLS using a PID controller (b) Control signal of PID controller.

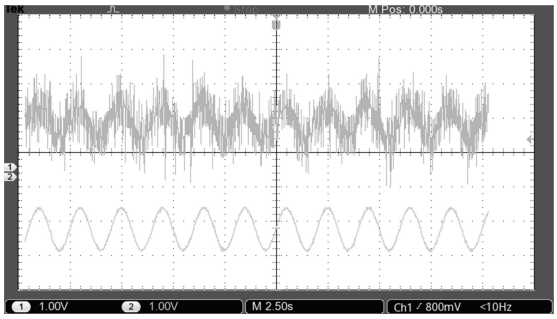

Fig. 18. Experimental PID controller output and object's trajectory captured on DSO.

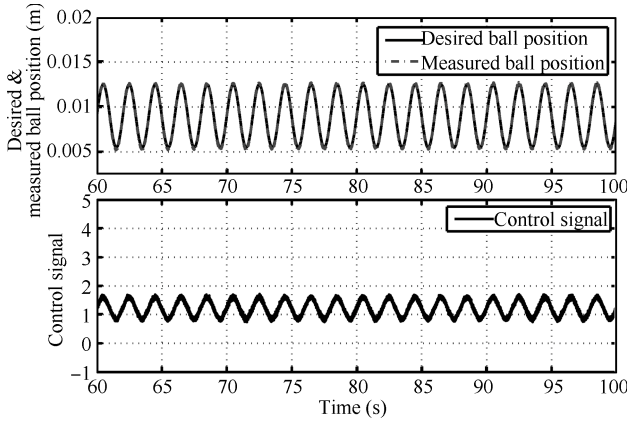

Fig. 19. (a) Controlled output result of MLS using a FO-PID controller (b) Control signal of FO-PID controller.

From the data presented in Table IV it is observed that FO-PID controller has improved the position accuracy of MLS compared to PD or PID controllers in real time implementation. Also, the percentage error is least for FO-PID controller.

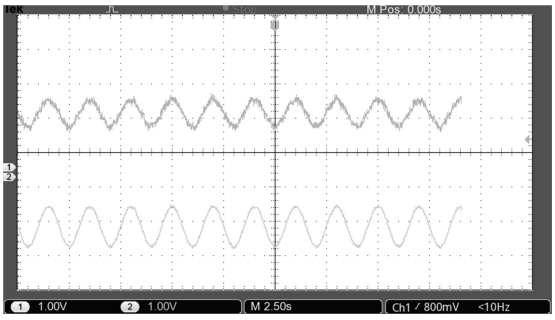

Fig. 20. Experimental FO-PID controller output and object's trajectory captured on DSO.

Table V
CONTROL EFFORT ANALYSIS OF DIFFERENT CONTROLLERS IN REAL TIME IMPLEMENTATION

Performance Indices		Controllers		
		PD	PID	FO-PID
IAE	Error Signal	51.97	14.56	12.79
	Control Signal	208	181	151.5
ITAE	Error Signal	609	455.7	425.5
	Control Signal	900.6	797.9	602.5
ISE	Error Signal	28.38	4.978	2.488
	Control Signal	832.6	647.2	347.2

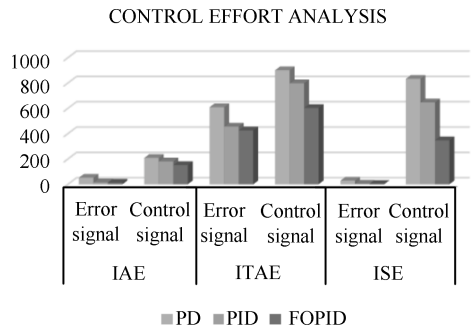

Fig. 21. Control effort analysis.

The control effort required by PD, PID, and FO-PID controllers is calculated using IAE (Integral Absolute Error), ITAE, and ISE (Integral Square Error). The analysis has been carried out for a period of $100s$ and is tabulated in Table V. Fig.21 represents the control effort analysis in pictorial form.

The error signal is maximum in the case of PD controller and least in the case of FO-PID controller. The control signal also follows the same pattern and is least in case of FO-PID controller, leading to inference that the control effort in terms of power required by the FO-PID controller to maintain the ball position is least amongst the three controllers.

From the analysis, it infers that PID controller is better than PD controller through performance characteristic. FO-PID controller shows slight improvement over PID controller, but the effort required is appreciably less for the same improvement. Thus proving superiority of FO-PID over integer order controllers.

4) Disturbance Injection Analysis of Controllers: The effect of disturbance is studied by injecting step input to MLS and effect of increased load is studied by introducing another metallic ball in levitation system as shown in Fig.22. The step is applied after interval of $25s$ on initiation of the input while another ball is introduced manually after $35s$. The measured and desired ball positions using a PD controller are presented in Fig.23(a) and the control signal of a controller is shown in Fig.23(b). PD controller output and object's trajectory as captured on DSO is presented in Fig.24.

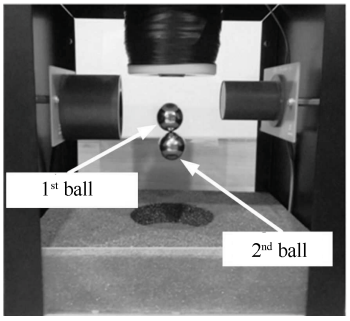

Fig. 22. Levitation of two metallic balls.

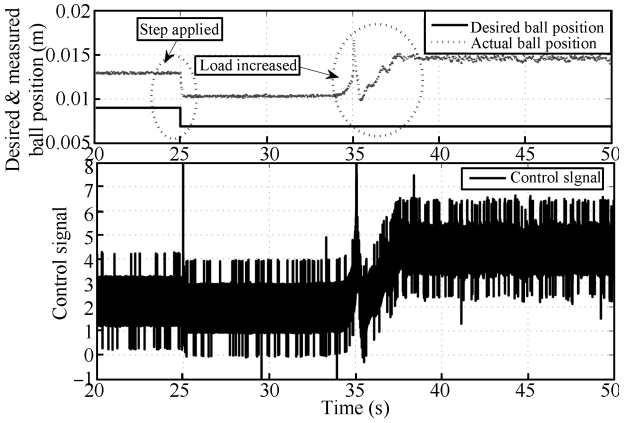

Fig. 23. (a) Controlled output result of MLS using a PD controller (b) Control signal of PD controller.

The instant of step applied in input signal and the instant of the addition of extra load are demonstrated by circles marked on figures. Overshoot is observed at the instant of step and after introducing second ball in levitation system.

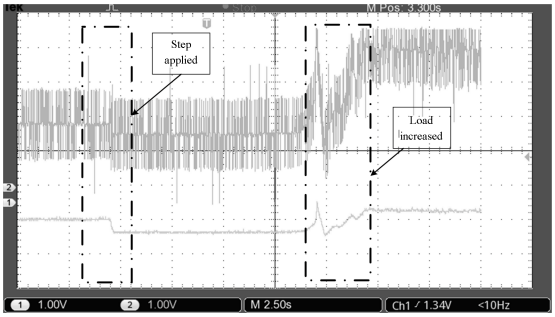

Fig. 24. Experimental PD controller output and object's trajectory captured on DSO.

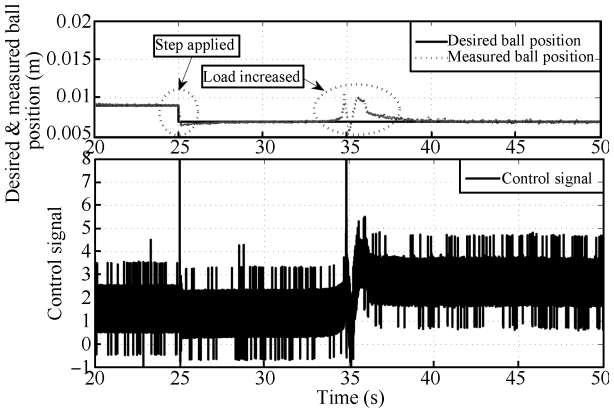

Fig. 25. (a) Controlled output result of MLS using a PID controller (b) Control signal of PID controller.

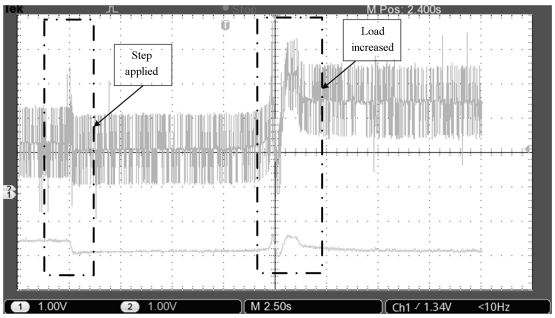

Fig. 26. Experimental PID controller output and object's trajectory captured on DSO.

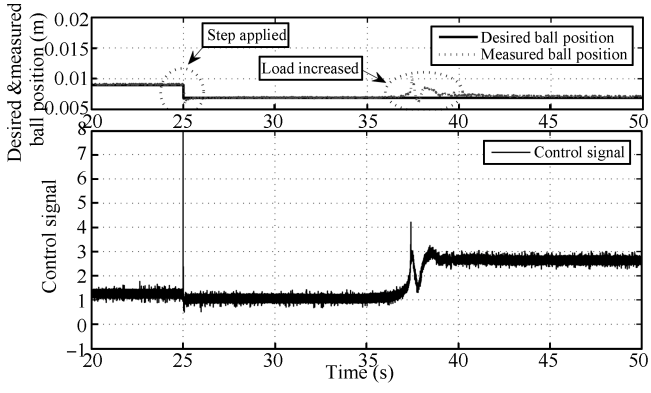

Fig. 27. (a) Controlled output result of MLS using a FO-PID controller (b) Control signal of FO-PID controller.

The deviation in ball position is higher as load is increased and greater amount of effort (power consumption, as indicated by high switching fluctuations in the voltage graph) is required by controller to achieve desired ball position.

Similar analysis for PID and FO-PID controllers is presented in Fig.25 - Fig.28. These figures lead to inference that in case of PID controller, the deviation in ball position is high and greater amount of effort is required by controller to achieve ball position as compared to FO-PID controller. Comparison shows that FO-PID controller requires lesser effort to levitate the object and effect of disturbance is less as compared to PD or PID controllers.

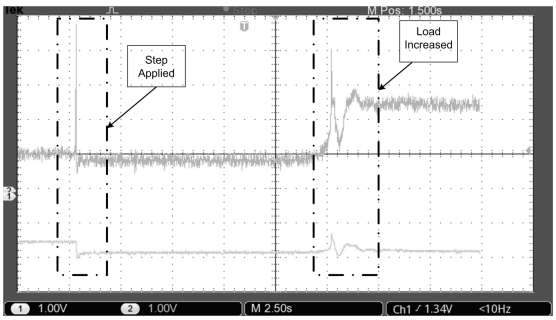

Fig. 28. Experimental FO-PID controller output and object's trajectory captured on DSO.

V. Conclusion

In this paper, digital FO-PID controller is applied on MLS to improve the positional accuracy and control effort. A new discrete optimal pole-zero approximation method is proposed for realization of controller. This method provides the optimal number of pole-zero pairs to maintain the phase value within the tolerance, of around 1^o. dPSO method is used for tuning the parameters of controller. The performance analysis for integer and fractional order controllers have been carried out in both simulation and experimentation. The results show that a better control over position accuracy with lesser efforts (over conventional methods) can be achieved. In practical terms, this efficiency improvement translates to better fuel efficiency. This paper provides a basis for evaluating the utility of fractional order control to improve the performance of power conversion systems and precision robotic applications.

Table VI
PARAMETERS OF THE MLS

Symbol	Parameters	Values
i	Input Current in the Coil	$[0-3]$A
u	Input Voltage	$[0-5]$V
m	Mass of the Steel Sphere	20×10^{-3} kg
k	Magnetic Constant	8.54×10^{-5} kg
k_1	Input Conductance	$0.3971/\Omega$
g	Gravitational Acceleration	$9.81m/s^2$

References

[1] C. M. Lin, M. H. Lin, and C. W. Chen, "SoPC-based adaptive PID control system design for magnetic levitation system," *IEEE Systems Journal*, Vol. 5, No. 2, pp. 278–287, June 2011. doi: 10.1109/JSYST.2011.2134530

[2] H. K. Chiang, C. A. Chen, and M. Y. Li, "Integral variable-structure grey control for magnetic levitation system," *IEE Proc. Electric Power Applications*, Vol. 153, No. 6, pp. 809–814, November 2006. doi: 10.1049/ip-epa:20060056

[3] Z. J. Yang, K. Kunitoshi, S. Kanae, and K. Wada, "Adaptive robust output-feedback control of a magnetic levitation system by K-filter approach," *IEEE Trans. on Industrial Electronics*, Vol. 55, No. 1, pp. 390–399, January 2008. doi: 10.1109/TIE.2007.896488

[4] R. Morales, V. Feliu, and H. Sira-Ramrez, "Nonlinear control for magnetic levitation systems based on fast online algebraic identification of the input gain," *IEEE Trans. on Control Systems Technology*, Vol. 19, No. 4, pp. 757–771, July 2011. doi: 10.1109/TCST.2010.2057511

[5] C. M. Lin, Y. L. Liu, and H. Y. Li, "SoPC-based function-link cerebellar model articulation control system design for magnetic ball levitation systems," *IEEE Trans. on Industrial Electronics*, Vol. 61, No. 8, pp. 4265–4273, August 2014. doi: 10.1109/TIE.2013.2288201

[6] A. El Hajjaji and M. Ouladsine, "Modeling and nonlinear control of magnetic levitation systems," *IEEE Trans. on Industrial Electronics*, Vol. 48, No. 4, pp. 831–838, August 2001. doi: 10.1109/41.937416

[7] R. C. Kluever, C. A. Kluever, *Dynamic Systems: Modeling, Simulation, and Control*, 1st Edition, John Wiley and Sons, April 2015.

[8] G. F. Franklin, J. D. Powell, and A. Emami-Naeini, *Feedback Control of Dynamic Systems*, 3rd Edition, Addison-Wesley, Reading, MA, 1994.

[9] T. H. Wong, "Design of a magnetic levitation control system - An undergraduate project," *IEEE Trans. on Education*, Vol. 29, No. 4, pp. 196–200, November 1986. doi: 10.1109/TE.1986.5570565

[10] R. Sinha and M. L. Nagurka, "Analog and labview-based control of a maglev system with NI-ELVIS," *ASME International Mechanical Engineering Congress and Exposition*, Orlando, Florida, USA, pp. 741–746, November 2005.

[11] S. Saha, S. Das, R. Ghosh, B. Goswami, R. Balasubramanian, A. K. Chandra, A. Gupta, "Design of a fractional order phase shaper for iso-damped control of a PHWR under step-back condition," *IEEE Trans. on Nuclear Science*, Vol. 57, No.3, pp. 1602–1612, June 2010. doi: 10.1109/TNS.2010.2047405

[12] S. Das, S. Das, and A. Gupta, "Fractional order modeling of a PHWR under step-back condition and control of its global power with a robust controller," *IEEE Trans. on Nuclear Science*, Vol. 58, No. 5, pp. 2431–2441, October 2011. doi: 10.1109/TNS.2011.2164422

[13] S. Saha, S. Das, R. Ghosh, B. Goswami, R. Balasubramanian, A. K. Chandra, S. Das, A. Gupta, "Fractional order phase shaper design with Bode integral for iso-damped control system," *ISA Trans.*, Vol. 49, No. 2, pp. 196–206, April 2010. doi:10.1016/j.isatra.2009.12.001

[14] S. Das, "Fuel efficient nuclear reactor control," *International Conference on Nuclear Engineering*, Beijing, China, May 16-20, 2005.

[15] K. J. Astrom and T. Hagglund, *PID Controllers: Theory, Design and Tuning*, Instrument Society of America, North Carolina, 1995.

[16] I. Podlubny, *Fractional Differential Equations*, Academic Press, New York, 1999.

[17] S. Das, (a) *Functional Fractional Calculus for System Identification and Controls*, Springer Science and Business Media, 2007, doi: 10.1007/978-3-540-72703-3; and (b) *Functional Fractional Calculus*, Springer Science and Business Media, 2011. doi: 10.1007/978-3-642-20545-3

[18] I. Podlubny, "Fractional-order systems and $PI^{\lambda}D^{\mu}$ controllers," *IEEE Trans. on Automatic Control*, Vol. 44, No. 1, pp. 208–214, January 1999. doi: 10.1109/9.739144

[19] A. Charef, H. H. Sun, Y. Y. Tsao, and B. Onaral, "Fractal system as represented by singularity function," *IEEE Trans. on Automatic Control*, Vol. 37, No. 9, pp. 14651470, September 1992. doi: 10.1109/9.159595

[20] A. Oustaloup, F. Levron, B. Mathiew, and F. M. Nanot, "Frequency-band complex noninteger differentiator: characterization and synthesis," *IEEE Trans. on Circuits and Systems I: Fundamental Theory and Applications*, Vol. 47, No. 1, pp. 25–39, January 2000. doi: 10.1109/81.817385

[21] Feedback Instruments Ltd., *Magnetic levitation control experiments, manual: 33-942S Ed01 122006*, Feedback Part No. 1160–33942S.

[22] R. Pintelon and J. Schoukens, *System Identification: A Frequency Domain Approach*, Wiley-IEEE Pres, ISBN 978-0-470-64037-1, 2012.

[23] C. Yeroglu and N. Tan, "Note on fractional-order proportional-integral-differential controller design," *IET Control Theory and Applications*, Vol. 5, No. 17, pp. 19781989, November 2011. doi: 10.1049/iet-cta.2010.0746

[24] D. Valerio and J. Sa da Costa, "Introduction to single-input, single-output fractional control," *IET Control Theory and Applications*, Vol. 5, No. 8, pp. 10331057, May 2011. doi: 10.1049/iet-cta.2010.0332

[25] D. Chen, Y. Q. Chen, and D. Xue, "Digital fractional order Savitzky-Golay differentiator," *IEEE Trans. on Circuits And Systems II: Express Briefs*, Vol. 58, No. 11, pp. 758–762, November 2011. doi: 10.1109/TCSII.2011.2168022

[26] M. O. Efe, "Fractional order systems in industrial automation-a survey," *IEEE Trans. on Industrial Informatics*, Vol. 7, No. 4, pp. 582–591, November 2011. doi: 10.1109/TII.2011.2166775

[27] J. A. T. Machado, "Discrete-time fractional-order controllers," *Fractional calculus and Applied Analysis*, Vol. 4, No. 1, pp. 47–66, January 2001.

[28] A. S. Dhabale, R. Dive, M. V. Aware, and S. Das, "A new method for getting rational approximation for fractional order differintegrals," *Asian Journal of Control*, Vol. 17, No. 6, pp. 21432152, November 2015. doi: 10.1002/asjc.1148

[29] Y. Q. Chen and K. L. Moore, "Discretization schemes for fractional-order differentiators and integrators," *IEEE Trans. on Circuits and Systems I: Fundamental Theory and Applications*, Vol. 49, No. 3, pp. 363–367, March 2002. doi: 10.1109/81.989172

[30] I. Pan and S. Das, *Gain and Order Scheduling for Fractional Order Controllers*, Intelligent Fractional Order Systems and Control, Springer Berlin Heidelberg, pp. 147157, 2013. doi: 10.1007/978-3-642-31549-7

[31] I. Petras, "Fractional order feedback control of a DC motor," *Journal of Electrical Engineering*, Vol. 60, No. 3, pp. 117128, March 2009.

[32] S. Cuoghi and L. Ntogramatzidis, "Direct and exact methods for the synthesis of discrete-time proportional-integral-derivative controllers," *IET Control Theory and Applications*, Vol. 7, No. 18, pp. 21642171, December 2013. doi: 10.1049/iet-cta.2013.0064

[33] Y. Q. Chen, I. Petras, and D. Xue, "Fractional order control-a tutorial," *American Control Conference*, St. Louis, MO, USA, June 10-12, pp. 1397–1411, 2009. doi: 10.1109/ACC.2009.5160719

[34] Y. Jin, Y. Q. Chen, and D. Xue, "Time-constant robust analysis of a fractional order [proportional derivative] controller," *IET Control Theory and Applications*, Vol. 5, No. 1, pp. 164172, January 2011. doi: 10.1049/iet-cta.2009.0543

[35] C. A. Monje, B. M. Vinagre, V. Feliu, and Y. Q. Chen, "Tuning and auto-tuning of fractional order controllers for industry applications," *Control Engineering Practice*, Vol. 16, No. 7, pp. 798812, July 2008. doi: 10.1016/j.conengprac.2007.08.006

[36] J. Zhong and L. Li, "Tuning fractional-order controllers for a solid-core magnetic bearing system," *IEEE Trans. on Control Systems Technology*, Vol. 23, No. 4, pp. 1648–1656, July 2015. doi: 10.1109/TCST.2014.2382642

[37] F. Padula and A. Visioli, "Optimal tuning rules for proportional-integral derivative and fractional-order proportional-integral-derivative controllers for integral and unstable processes," *IET Control Theory and Applications*, Vol. 6, No. 6, pp. 776786, April 2012. doi: 10.1049/iet-cta.2011.0419

[38] S. Das, S. Saha, S. Das, and A. Gupta, "On the selection of tuning methodology of FOPID controllers for the control of higher order processes," *ISA Transactions*, Vol. 50, No. 3, pp. 376–388, July 2011. doi: 10.1016/j.isatra.2011.02.003

[39] S. Das, I. Pan, S. Das, and A. Gupta, "A novel fractional order fuzzy PID controller and its optimal time domain tuning based on integral performance indices," *Engineering Applications of Artificial Intelligence*, Vol. 25, No. 2, pp. 430–442, March 2012. doi: 10.1016/j.engappai.2011.10.004

[40] S. Das, I. Pan, S. Das, and A. Gupta, "Improved model reduction and tuning of fractional-order $PI^{\lambda}D^{\mu}$ controllers for analytical rule extraction with genetic programming," *ISA Transactions*, Vol. 51, No. 2, pp. 237–261, March 2012. doi: 10.1016/j.isatra.2011.10.004

[41] S. Das, I. Pan, K. Halder, S. Das, and A. Gupta, "LQR based improved discrete PID controller design via optimum selection of weighting matrices using fractional order integral performance index," *Applied Mathematical Modelling*, Vol. 37, No. 6, pp. 4253–4268, March 2013. doi: 10.1016/j.apm.2012.09.022

[42] S. Das, I. Pan, and S. Das, "Performance comparison of optimal fractional order hybrid fuzzy PID controllers for handling oscillatory fractional order processes with dead time," *ISA Transactions*, Vol. 52, No. 4, pp. 550–566, July 2013. doi: 10.1016/j.isatra.2013.03.004

[43] S. Das, I. Pan, S. Das, and A. Gupta, "Master-slave chaos synchronization via optimal fractional order $PI^{\lambda}D^{\mu}$ controller with bacterial foraging algorithm," *Nonlinear Dynamics*, Vol. 69, No. 4, pp. 2193–2206, September 2012. doi: 10.1007/s11071-012-0419-x

[44] S. Saha, S. Das, S. Das, and A. Gupta, "A conformal mapping based fractional order approach for sub-optimal tuning of PID controllers with guaranteed dominant pole placement," *Communications in Nonlinear Science and Numerical Simulation*, Vol. 17, No. 9, pp. 3628–3642, September 2012. doi: doi:10.1016/j.cnsns.2012.01.007

[45] S. Das, I. Pan, K. Halder, S. Das, and A. Gupta, "Impact of fractional order integral performance indices in LQR based PID controller design via optimum selection of weighting matrices," *IEEE International Conference on Computer Communication and Informatics*, Coimbatore, India, Jan. 1012, pp. 1–6, 2012. doi: 10.1109/ICCCI.2012.6158892

[46] S. Das, I. Pan, S. Das, and A. Gupta, "Genetic algorithm based improved sub-optimal model reduction in nyquist plane for optimal tuning rule extraction of PID and $PI^{\lambda}D^{\mu}$ controllers via genetic programming," *IEEE International Conference on Process Automation, Control and Computing*, July 20, pp. 1–6, 2011. doi: 10.1109/PACC.2011.5978962

[47] A. Rajasekhar, S. Das, and A. Abraham, "Fractional order PID controller design for speed control of chopper fed DC motor drive using artificial bee colony algorithm," *IEEE World Congress on Nature and Biologically Inspired Computing*, August 12, pp. 269–266, 2013. doi: 10.1109/NaBIC.2013.6617873

[48] R. Song and Z. Chen, "Design of PID controller for maglev system based on an improved PSO with mixed inertia weight," *Journal of Networks*, Vol. 9, No. 6 , pp. 1509–1517, January 2014. doi: 10.4304/jnw.9.6.1509-1517

[49] A. Q. Badar, B. S. Umre, and A. S. Junghare, "Reactive power control using dynamic particle swarm optimization for real power loss minimization," *International Journal of Electrical Power and Energy Systems*, Vol. 41, No. 1, pp. 133136, Octomber 2012. doi: 10.1016/j.ijepes.2012.03.030

Amit S. Chopade (S'16) received the B.E. degree from Nagpur University, India, in 2012. Currently, he is working as Junior Research Fellow on BRNS Research Project "Development of Industrial Fractional Order PID Controller" at Visvesvaraya National Institute of Technology, Nagpur, India.

His research interests include electrical drives, energy efficient systems, and applications of fractional order controllers.

Swapnil W. Khubalkar (S'15) received the B.E. and M.Tech degree from Nagpur University, India, in 2010 and 2012, respectively. Currently he is working toward Ph.D. in the area of fractional order controllers at Visvesvaraya National Institute of Technology, Nagpur, India.

His research interests include electrical drives, controls, and applications of fractional order controllers.

Anjali S. Junghare received the B.E. and M.Tech degree from Visvesvaraya Regional College of Engineering (VRCE), Nagpur, India, in 1981 and 1985, respectively. She received the Ph.D. degree from VRCE in 2007. She is currently an associate professor in the Department of Electrical Engineering, Visvesvaraya National Institute of Technology, Nagpur, India. She has 13 years of industrial experience and 19 years of academic experience.

Her research areas are control system, fractional order controllers, fuzzy Logic and its applications.

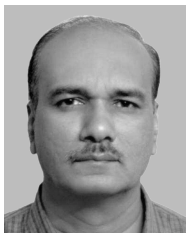

Mohan V. Aware (M'08, SM'14) received the B.E. degree in Electrical Engineering from College of Engineering, Amravati, India, in 1980, the M.Tech degree from the Indian Institute of Technology, Bombay, in 1982 and the Ph.D. degree for research work on "Direct Torque Controlled Induction Motor Drives" from Nagpur University, India, in 2002. From 1982 to 1989, he was a Design Officer with Crompton Greaves Ltd., Nasik, India. From 1989 to 1991, he was a Development Engineer with Nippon Denro India pvt. Ltd. During 2001-2002, he was a Research fellow with Electrical Engineering Department, Hong Kong Polytechnic University, Hong Kong. Presently, he is a Professor in Electrical Engineering Department, Visvesvaraya National Institute of Technology, Nagpur, India.

His research areas are electrical drives, distributed generation with energy storage and power electronics. He has published more than 150 technical papers in different journals and conferences.

Shantanu Das works as a Scientist Bhabha Atomic Research Centre(BARC), India. He graduated in Electrical Engineering and Electronics Engineering, from BITS Pilani and thereafter working as scientist at BARC, since 1984, in the area of Nuclear Reactor Control and Safety. He is doing development on Fractional Calculus since about 1998, in order to understand natural laws and to engineer for betterment in controls, signal processing and systems identification. Since 2004, he is working on development of meta-material science to understand exotic properties of electro magnetism and to manipulate electromagnetic flow for usage is electronics systems, and also in application of microwave power for material processing. He is Honorary Senior Research Professor at Department of Physics, Jadavpur University, Adjunct Professor at DIAT Pune, and under UGC Visiting Fellow at Department of Applied Mathematics, Calcutta University. He has several publications and patents on all these topics.